



# Human platelet lysate (hPL) alters the lineage commitment and paracrine functions of human mesenchymal stem cells via mitochondrial metabolism

Ping Du<sup>a</sup>, Xuelian Tao<sup>a</sup>, Kun Liu<sup>a</sup>, Jiao Lin<sup>a</sup>, Yue Shi<sup>a</sup>, Kwideok Park<sup>b</sup>, Hsien-Yeh Chen<sup>c</sup>, Chao-Po Lin<sup>d</sup>, Junlei Chang<sup>a</sup>, Raymond CB Wong<sup>e,f</sup>, Haobo Pan<sup>a</sup>, Peng-Yuan Wang<sup>a,g,h,\*</sup>

<sup>a</sup> Shenzhen Key Laboratory of Biomimetic Materials and Cellular Immunomodulation, Shenzhen Institute of Advanced Technology, Chinese Academy of Sciences, Shenzhen, Guangdong 518055, China

<sup>b</sup> Center for Biomaterials, Korea Institute of Science and Technology (KIST), Seoul 02792, South Korea

<sup>c</sup> Department of Chemical Engineering, National Taiwan University, Taipei 110, Taiwan

<sup>d</sup> School of life science and technology, Shanghai Technology University, Shanghai, China

<sup>e</sup> Centre for Eye Research Australia, Royal Victorian Eye and Ear Hospital, Australia

<sup>f</sup> Ophthalmology, Department of Surgery, University of Melbourne, Australia

<sup>g</sup> Department of Chemistry and Biotechnology, Swinburne University of Technology, Hawthorn, Victoria 3122, Australia

<sup>h</sup> Oujiang Laboratory, Wenzhou, Zhejiang 325000, China

## ARTICLE INFO

### Article history:

Received 19 July 2021

Revised 27 October 2021

Accepted 7 November 2021

Available online 4 December 2021

### Keywords:

Human platelet lysate

Mesenchymal stem cell

Lineage commitment

Mitochondrial metabolism

Paracrine functions

## ABSTRACT

Emerging evidence indicates that cellular bioenergetics is critical in determining the self-renewal and differentiation of stem cells. Human platelet lysate (hPL) contains abundant proteins, which has been shown to improve self-renewal and osteogenic differentiation of mesenchymal stem cells (MSCs). However, the detailed modulating effect of hPL on MSCs energy metabolism remains unexplored. This study showed that MSCs cultured in hPL displayed a reduced cell size and cell spreading, but an improved proliferation and osteogenic capability compared with cells maintained in fetal bovine serum (FBS). RNA sequencing revealed widespread transcriptome differences between hPL- and FBS-MSCs where the differential expressed genes (DEGs) were enriched mainly in the PI3K-Akt and metabolic signal pathways. We found a significant downregulation of HIF1A (hypoxia-inducible factor 1 alpha) and altered mitochondrial features in hPL-MSCs, indicating a metabolism switch of the hPL-treated cells from glycolysis towards mitochondrial oxidative phosphorylation (OxPhos). It was also demonstrated that hPL-MSCs tend to differentiate towards the aerobic metabolism-demanded osteocytes or adipocytes rather than the anaerobic metabolism-demanded chondrocytes using a differentiation medium. Finally, hPL-MSCs showed an impaired paracrine function where the secreted factors cannot stimulate M2 polarization of THP1 cells and angiogenesis of HUVECs. We concluded that the PI3K-Akt/HIF1A-mediated metabolic state dominated the physiological property and lineage commitment of MSCs in hPL. For the first time, this study demonstrates the molecular mechanism of hPL in the regulation of metabolism and functions of MSCs, which implies the potential of hPL as an efficient biological material for stem cell engineering and regenerative medicine.

© 2021 Elsevier Ltd. All rights reserved.

## 1. Introduction

Human mesenchymal stem cells (MSCs) show great promise for cell therapy, tissue engineering, and regenerative medicine due to their self-renewal, multipotency [1], and paracrine functions [2]. MSCs exist in various tissues; however, they are relatively rare. Therefore, the therapeutic application of MSCs requires an *ex*

*vivo* expansion to get a clinically significant cell number [3]. Fetal bovine serum (FBS) has long been the gold standard medium supplement for laboratory-scale MSCs culture. However, FBS has a poorly characterized composition and poses risk factors, as it may be a source of xenogenic antigens and zoonotic infections [4]. For these reasons, an alternative is imperative for the *ex vivo* expansion of MSCs. Different alternatives, including chemically-defined media and human blood derivatives, have been developed recently. Chemically-defined media generally consist of basic media supplemented with different kinds of recombinant proteins or growth

\* Corresponding author.

E-mail address: [pywang0624@gmail.com](mailto:pywang0624@gmail.com) (P.-Y. Wang).

factors, which are nowadays commercially available. However, the development of cell-specific chemically-defined media is expensive and time-consuming, as MSCs property varies with their sources and donors [5]. Therefore, the autologous or allogeneic human serum has been developed for *ex vivo* expansion of MSCs [4, 6].

Human platelet lysate (hPL) is emerging as an attractive serum alternative, as platelet contains abundant bioactive molecules and growth factors, and they play an essential physiological role in wound healing and tissue repair [7]. Since the first study in 2005 describing the preparation and use of hPL for MSCs expansion [8], a series of reports have shown that both allogeneic and autologous hPL is superior to FBS for stimulating the expansion of MSCs derived from bone marrow [9], umbilical cord blood [10], and adipose tissue [11]. Reports have also found that hPL can maintain the stemness of MSCs [12] and support their multipotency toward osteoblasts [13], chondrocytes, and adipocytes [14, 15]. The promotive effect of hPL on cell expansion is likely attributed to the high concentrations of growth factors within platelets, such as platelet-derived growth factor (PDGF), fibroblast growth factor (FGF), insulin-like growth factor (IGF), transforming growth factor-beta (TGF-beta), platelet factor 4 (PF-4), and platelet-derived epidermal growth factor (PD-EGF) [16, 17]. Studies have demonstrated that hPL could maintain the self-renewal, multipotency, and immunophenotypes of MSCs; however, it is still controversy over whether the hPL-expanded MSCs (hPL-MSCs) retain their immunosuppressive properties. Some studies demonstrated a therapeutic effect of hPL-MSCs on graft-versus-host diseases [18], whereas others concluded that hPL-MSCs have an inferior immunosuppressive capability [19, 20]. Also, it was suggested that the variability of donor selection and hPL manufacturing lead to the inconsistency of some results [21].

Furthermore, hPL-derived biomaterials have been widely explored as cost-effective sources for tissue engineering applications (e.g. hPL can be crosslinked or blended with other proteins or polysaccharides to form hydrogels, scaffolds, and patches). The use of platelet-derived materials in regenerative medicine has different advantages such as they can be either autologous or allogeneic, and they exhibit a modulatory effect on both inflammatory and wound healing processes [22, 23].

Previous studies have focused on the effect of hPL on the expansion and application of MSCs, however, the modulating mechanism of hPL on the cellular properties and metabolic state of MSCs is unclear. Given the great impact of hPL on the multipotency and immunomodulatory property of MSCs, we hypothesized that hPL participates the metabolism of MSCs. The purpose of this study is to interpret the transcriptional correlation with the biological properties of MSCs in hPL in terms of cell adhesion, morphology, metabolic activity, ECM secretion, differentiation, and paracrine function. Comprehensive characterization of the function and phenotype of MSCs using various concentrations of hPL is essential for clinical application of hPL-MSCs. In addition, understanding the function of hPL on MSCs will benefit the development of new strategies to use hPL and hPL-MSCs in tissue engineering and regenerative medicine.

## 2. Materials and methods

### 2.1. Cell culture

Human fetal bone marrow mesenchymal stem cells (fBMSCs) were purchased from Cyagen Biosciences (HUXMF-01,001, Suzhou Inc.) at passage 2. Cells were routinely maintained in complete growth media (HUXMF-90,011, Cyagen Bioscience). Human adult bone marrow mesenchymal stem cells (aBMSCs) were purchased from Lonza (PT-2501) and maintained according to the manufacturer's instruction. Human adipose-MSCs (ASC, passage 2) were

purchased from Cyagen Bioscience (HUXMD-01,001), and they were maintained in complete growth media (HUXMD-90,011) with 100 U/mL penicillin, and 100 µg/mL streptomycin (Invitrogen, Carlsbad, CA). THP-1 cells (ATCC TIB®-202™) were kindly provided by Stem Cell Bank, Chinese Academy of Sciences, and maintained in RPMI-1640 media supplemented with 10% FBS and antibiotics. HUVECs purchased from ATCC (ATCC® PCS-100-013™) were maintained in a vascular cell basal medium (ATCC® PCS-100-030) supplemented with an endothelial cell growth kit (ATCC PCS-100-041). All cells were cultured at 37 °C under a 5% CO<sub>2</sub> humidified atmosphere.

To investigate different media formulation effects on MSCs behaviors, MSCs were cultured in MEM-α media (Gibco, C12571500BT) supplemented with either 10% fetal bovine serum (FBS, Hyclone, SH30406.02, New Zealand), or various concentrations of human platelet lysate (hPL, HPCFDCL10, UltraGRO™ Advanced, Helios BioScience).

### 2.2. Cell proliferation and activity

The cell activity of fBMSCs in different media formulations was first examined at 3, and 48 h post-cell seeding via Cell Counting Kit-8 (CC0039, Beyotime Biotechnology). In brief, fBMSCs were seeded in 24-well plate ( $n = 5$ ) at a density of 5000 cells/cm<sup>2</sup> in media with different concentrations (1, 2, 3, 4, and 5%, v/v) of hPL, and media with 10% FBS was the control. The CCK-8 assay was carried out at least for three repeats.

Cell proliferation level of fBMSCs in 1–5% hPL and 10% FBS ( $n = 5$ ) at day 4 was then examined via Quant-iT™ PicoGreen ds-DNA Assay Kit (P7589, ThermoFisher). The cell numbers and cell sizes of fBMSCs in different media were also compared at various time points ( $n = 5$ ), which was determined using an automatic cell counter (luna-II Autofocus Cell Counter, South Korea).

### 2.3. Osteogenic and chondrogenic differentiation

fBMSCs were plated in multi-well plates at a density of  $2 \times 10^4$  cells/cm<sup>2</sup> and maintained in growth media (GM, MEM-α media with 10% FBS) until confluence ( $n = 3$ ). For osteogenic induction (OI), the GM were switched to the OI media (MEM-α media with 2%, 5% hPL, or 10% FBS, respectively, and with the OI reagents of 10 nM dexamethasone, 10 mM β-glycerophosphate, and 50 µg/mL ascorbic acid-2 phosphate (Sigma-Aldrich)). For chondrogenic induction (CI), the GM were switched to the CI media (high glucose DMEM with 0, 2%, 5% hPL, or 2% FBS, respectively, and with the CI reagents of 10 nM dexamethasone, 10 ng/mL transforming growth factor-beta1 (TGF-beta1, Prospec), 50 µg/mL ascorbic acid-2 phosphate, 40 µg/mL L-proline, 1.25 mg/mL bovine serum albumin, 1% insulin-transferrin-selenium (ITS, Gibco), 1 mM sodium pyruvate (Gibco, Grand Island, NY, USA)). The media were replenished every other day.

### 2.4. Immunofluorescence staining

For cell morphology and focal adhesion staining, fBMSCs were seeded in 2%, 5% hPL and 10% FBS media ( $n = 3$ ) at a density of 5000 cells/cm<sup>2</sup> on glass coverslips (14 mm-diameter) plated in 24-well plate and fixed after 48 h. The primary antibody of mouse monoclonal anti-vinculin (v9131; Sigma-Aldrich, 1: 400) and secondary antibody of goat anti-mouse IgG-H&L FITC (ab6785) were employed for vinculin staining. Phalloidin-Rhodamine B (P1961, Sigma-Aldrich) was employed for F-actin filament staining. Samples were washed thoroughly and mounted via Fluoroshield Mounting Medium with DAPI (ab104139). Vinculin puncta (dots per cell) and cell morphology (aspect ratio and

spreading area) were quantified using Image J software (a minimum of 50 cells were analyzed).

For type I collagen (COL1A1) staining, fBMSC were cultured in GM for 10 days and in OI media for 14 days, respectively. Samples were fixed, washed thoroughly and stained with the primary antibody of COL1A1 (ab34710, 1: 500 dilution) and then with a secondary antibody of donkey anti-rabbit IgG H&L Alexa Fluor 488® (ab150073, 1: 1000 dilution). Images were acquired using inverted fluorescence microscopy (Olympus, Japan).

### 2.5. ALP assay

The alkaline phosphatase (ALP) activity of fBMSC after osteogenic differentiation ( $n = 3$ ) for 4- and 7-days was quantitatively and semi-quantitatively assessed using an ALP assay kit (P0321, Beyotime Biotechnology) and BCIP/NBT Alkaline Phosphatase Color Development Kit (C3206, Beyotime Biotechnology), respectively. For quantitative analysis ( $n = 5$ ), cells were lysed using the RIPA Lysis Buffer (P0013C), collected and centrifuged at 14,000 g for 10 min at 4 °C. The supernatant was collected for ALP quantification according to the manufacturer's instructions. ALP levels in different groups were normalized by dividing the total protein determined by BCA assay (P0009, Beyotime Biotechnology). For semi-quantitative examination of ALP activity, cells were fixed by 4% paraformaldehyde (PFA) for 10 min, washed by PBS for 3 times, and subjected to ALP staining. In brief, samples were incubated with the freshly prepared staining solution for 30 min, and the reaction was terminated via rinsing with distilled water. The stained samples were captured using an inverted microscope.

### 2.6. Alizarin Red S assay

Cells were fixed with 4% PFA after osteogenic differentiation for different periods. Samples were washed thoroughly and stained with 1% Alizarin Red S (Sigma-Aldrich) solution (pH is 4.2 in Triz-HCL) for 15 min at room temperature. Afterwards, samples were thoroughly washed with deionized water for three times and examined under a bright-field microscope. Additionally, Alizarin Red S stained samples ( $n = 3$ ) were further extracted via 10% (w/v) cetylpyridinium chloride (Sigma-Aldrich, PHR1226) in PBS. The absorbance of the supernatant was read at 590 nm using a Multiskan Microplate Reader (Thermo Scientific). The experiments were carried out for at least three times.

### 2.7. Alcian blue staining and GAG assay

After chondrogenic differentiation for 4 weeks (4 W), fBMSCs were fixed for alcian blue (A3157) staining to compare the glycosaminoglycan (GAG) deposition levels in different media; meanwhile, samples were harvested at 2- and 4-W for quantitative measurement of GAG contents. In brief, samples were washed with PBS, harvested with 1 mg/mL papain in 0.1 M phosphate buffer with 10 mM L-cysteine hydrochloride and 10 mM Na<sub>2</sub>EDTA, and then digested for 16 h at 56 °C to release the GAG. The total GAG content of each sample ( $n = 3$ ) was measured spectrophotometrically at 530 nm using 1,9-dimethyl methylene blue (DMB) dye, along with the use of chondroitin sulfate as a standard. The total GAG content was then normalized to the amount of DNA in each sample lysate, which was determined via a Quant-iT™ PicoGreen™ dsDNA quantitation assay kit (P11496, Invitrogen).

### 2.8. RNA sequencing

fBMSC cultured in GM with 5% hPL or 10% FBS for 7 days, and fBMSCs cultured in GM with 5% hPL or 10% FBS for 7 days followed by an additional 7-day culture in OI media were named as hPL-7d,

FBS-7d, hPL-14d, and FBS-14d (Fig. S2), respectively. Samples were extracted using Trizol (Invitrogen) according to the manufacturer's instructions. The samples were analyzed via a HiSeq3000 platform, and the differently expressed genes (DEG, Q value < 0.05, |log<sub>2</sub>(fold change)| > 1) genes were assessed by DEseq using read counts as the input. Kobas 3.0 was used for KEGG and GO enrichment analysis calculated using Fisher's exact test with an FDR correction via Benjamini and Hochberg method.

### 2.9. HIF1A expression

For transcriptional level examination of HIF1A in fBMSCs, cells were cultured in 5% hPL and 10% FBS for 7 days, and they were harvested by Trizol reagents for total mRNA extraction and qRT-PCR analysis.

For intracellular HIF1A protein level examination, fBMSCs were cultured in 5% hPL and 10% FBS for 7 days, and harvested using the RIPA Lysis Buffer with the supplement of 3 mM EDTA and protease inhibitor cocktails (P8304, Sigma Aldrich). The cell lysates were centrifuged, and the supernatant was used freshly for HIF1A level examination using a human/mouse HIF1A-ELISA kit (PH368, Beyotime Biotechnology). The protein level of HIF1A was then normalized by dividing the DNA amount determined by a DNA quantitation assay kit (P11496, Invitrogen).

### 2.10. Mitochondria characterization

To investigate the effect of different media supplements on MSCs (fBMSCs and ASCs) mitochondrial morphology, cells were seeded in 24-well plates at a cell density of 2 000 cells/cm<sup>2</sup> and cultured in 5% hPL and 10% FBS for 7 days ( $n = 5$ ), respectively. The mitochondria were stained by Mito-Tracker Green (C1048, Beyotime Biotechnology). In brief, the Mito-Tracker Green was added into a freshly prepared cell growth media at a concentration of 200 nM and incubated for 45 min, and then the mitochondrial structures were observed under a fluorescence microscope.

### 2.11. Mitochondrial membrane potential

JC-1 mitochondrial membrane potential assay kit (C2006, Beyotime Biotechnology) was used to measure mitochondrial membrane potential following the manufacturer's protocol. In brief, MSCs (fBMSCs and ASCs) were cultured in 5% hPL and 10% FBS media for 7 days, and they were analyzed as adhered and suspended cells ( $n = 3$ , each), respectively. For adhered cell staining, cells were cultured on gelatin pre-coated glass coverslips; they were washed and then incubated with JC-1 staining solution. The fluorescence of each sample was observed under a fluorescence microscope. For cell suspensions, cells were trypsinized, harvested into the tube and incubated with JC-1 staining solution (1 μM) at 37 °C for 20 min in the dark. The cells were washed and resuspended in growth media. JC-1 signal was detected from FL1 and FL2 channels by a FACS flow cytometer (Invitrogen Attune Nxt, Thermo Fisher). The MSCs treated by 50 μM CCCP for 5 min were served as the zero-potential control. The fluorescence of the test samples was analyzed immediately after the preparation.

### 2.12. The immunomodulatory and angiogenic capacity

After a 7-day culture in 5% hPL or 10% FBS, the media of fBMSCs (P7 or P8) were replenished with serum-free RPMI-1640 media (Gibco, 11,875,093) and cultured for 48 h for condition media (CM) collection. The collected CM were centrifuged and used freshly for the functional activity tests (4 batches of conditioned media were used). The immunomodulatory effect of the CM was

evaluated using both resting macrophages (M0) and classical active macrophages (M1), respectively. In brief, THP-1 monocytes ( $1 \times 10^5$  cells/well in 24-well plate) were induced to the adhesive M0 macrophages with 50 ng/mL phorbol 12-myristate 13-acetate (PMA, P1585, Sigma-Aldrich) for 24 h; M0 macrophages were stimulated to M1 macrophages using LPS (1  $\mu$ g/mL, Sigma-Aldrich) and IFN- $\gamma$  (20 ng/mL, PeproTech). The CM of FBS- and hPL-cultured fBMSCs (FBS-CM and hPL-CM) were added to M0 or M1 macrophages for 24 h ( $n = 5$ ), respectively, with the serum-free RPMI-1640 media as control. The macrophage phenotypes after CM treatment were assessed via protein quantification of TNF- $\alpha$  and IL-10 using the ELISA kit (SinoBiological).

The angiogenic effect of CM was evaluated via HUVECs tube formation and proliferation assay, respectively. For tube formation assay, HUVECs were seeded in CM on Matrigel® (354,262, Corning, 1:3 dilution)-coated 96-well plate at a cell density of  $1 \times 10^4$  cells/well ( $n = 5$ ), and the tube formation levels were compared by quantification of the total segment length using the angiogenesis analyzer Plugin (Image J software). For cell proliferation assay, HUVECs were seeded in each CM, serum-free RPMI-1640 (negative control), and the standard endothelial growth medium (EGM, positive control) in 96-well plate (5 000 cells/well,  $n = 5$ ), respectively. HUVECs proliferation level was compared by CCK-8 assay at 24 h.

### 2.13. Real-time RT-PCR

Total mRNA was extracted using Trizol (15,596, ThermoFisher Scientific) at various conditions. The extracted mRNA was used for cDNA synthesis using a Transcript First Strand cDNA synthesis kit (Takara, RR037A). PCR was performed using 2X Real Star Power SYBR Mixture (Genestar, A311). The PCR reaction was performed using a Real-Time PCR System (Biorad, CFX96 Touch). Glyceraldehyde 3-phosphate dehydrogenase (GAPDH) was used as internal control, and transcript levels were calculated using the comparative ddCt method. Target genes and designed primer sequences were listed in table S1.

### 2.14. Statistical analysis

Statistical analyses of the data are performed using a one-way analysis of variance (ANOVA), with Tukey's post-hoc multiple comparisons (GraphPad Prism 8). All of the data represent the mean values and standard deviations. Statistical significance was expressed as \*( $p < 0.05$ ), \*\*( $p < 0.01$ ), or \*\*\*( $p < 0.001$ ).

## 3. Results

### 3.1. hPL decreased cell size and promoted cell growth

fBMSCs were able to adhere and grow in different concentrations of hPL (1%–5%), but they were slightly different in cell morphology and cell density (Fig. 1A). Cell morphological analysis exhibited that cell spreading areas, aspect ratios, and cell sizes vary with hPL concentrations. Interestingly, fBMSCs showed a smaller spreading area in all hPL concentrations (Fig. 1B), while cell elongation was inversely correlated with hPL concentrations (Fig. 1C); furthermore, the average cell diameter of the harvested fBMSCs (in suspension) after a 4-day expansion in 5% hPL was about 13.1  $\mu$ m that was significantly smaller than those harvested from 2% hPL (~14.24  $\mu$ m) or 10% FBS media (~15.14  $\mu$ m, Fig. 1D).

The CCK-8 assay demonstrated that fBMSCs had similar metabolic activity in different media after 3 h-culture, but that was inversely correlated with the hPL concentrations after 48 h (Fig. 1E). On the other hand, DNA quantification showed hPL promoted fBMSCs proliferation in a dose-dependent manner, and the DNA amount of cells in 5% hPL was 1.30-folds of that in 10% FBS at

day 4 (Fig. 1F). In addition, the cell counting showed that the cell number in 5% hPL was 1.75-folds of that in FBS control on day 4 (Fig. 1G).

The images of vinculin and F-actin staining exhibited that focal adhesion and cell spreading area of fBMSCs was reduced in 5% hPL compared to those in the FBS control (Fig. 1H). In addition, the average number of vinculin puncta per cell in 5% hPL was about 20% less than that in the FBS control (Fig. 1I).

### 3.2. hPL enhanced osteogenic differentiation

After a 4-day osteogenic differentiation, ALP activity of fBMSCs in 2% and 5% hPL was significantly higher than those in the FBS control. The ALP activity of fBMSCs was declined after a 7-day differentiation in both hPL and FBS; however, that in 2% hPL-treated cells maintained a significantly higher level than those in the FBS control (Fig. 2A and 2B). Transcript examination showed that fBMSCs cultured in GM with 2% hPL or 5% hPL for 7 days expressed significantly higher levels (2.0- and 1.7-folds, respectively) of ALP than those in the 10% FBS media. Further, after 1W- and 2W-osteogenic differentiation, the transcript level of ALP in 2% hPL-fBMSCs was significantly higher than that in 5% hPL and 10% FBS (Fig. 2C).

The images and the semi-quantitative analysis of ARS staining demonstrated visible matrix mineralization in all the test groups as early as day 9, and hPL induced a more substantial mineralization effect than FBS at later time points (after day 12, Fig. 2D and 2E). Further, the higher expression level of OCN (osteocalcin, BGLAP) in hPL-fBMSCs, a marker for osteoblast maturation, after a 3W-osteogenic differentiation indicated the advanced osteogenic effect of hPL over FBS control (Fig. 2F).

In GM, the orientation of the packed COL1A1 fibers in hPL-fBMSCs was very different from those in FBS-cultured cells. Interestingly, COL1A1 seems to be degraded after osteogenic differentiation (Fig. 2G and Fig. S1A). Similarly, the transcript level of COL1A1 was significantly lower in 5% hPL-fBMSCs than these in the other groups in both growth and OI media (Fig. 2H).

### 3.3. hPL enhanced matrix mineralization

ALP staining showed a higher ALP activity of all MSC origins grown in 5% hPL than those in 10% FBS after a 3-day osteogenic differentiation, and the trend maintained until 6 days except for the aBMSCs. ARS staining of 24-well insert clearly showed that 5% hPL induced a more advanced matrix mineralization effect on all MSCs than the FBS control after a 10-day osteogenic differentiation (Fig. 3A and 3B). In addition, the semi-quantitative results of the ARS staining showed that the matrix mineralization efficiency of hPL on MSCs slightly varies with the origins of MSCs, higher on bone marrow-MSC (aBMSCs and fBMSCs) and lower on ASC. Taken together, 5% hPL exhibited a better osteogenic effect than that of 10% FBS on all the MSCs (Fig. 3C).

### 3.4. hPL suppressed chondrogenic differentiation

Alcian blue staining of fBMSCs after a 4-week chondrogenic differentiation exhibited that the addition of either hPL or FBS into the CI media induced cell aggregates formation during culture, which makes it difficult to compare the staining levels among different samples (Fig. 4A). The normalized glycosaminoglycan level (GAG/DNA;  $\mu$ g/ $\mu$ g) showed that either hPL or FBS failed to enhance fBMSCs chondrogenesis (Fig. 4B). Gene examination of chondrogenic markers further confirmed the inhibition effect of hPL and FBS on fBMSCs chondrogenesis, and the inhibition effect of hPL was dose-dependent (Fig. 4C).

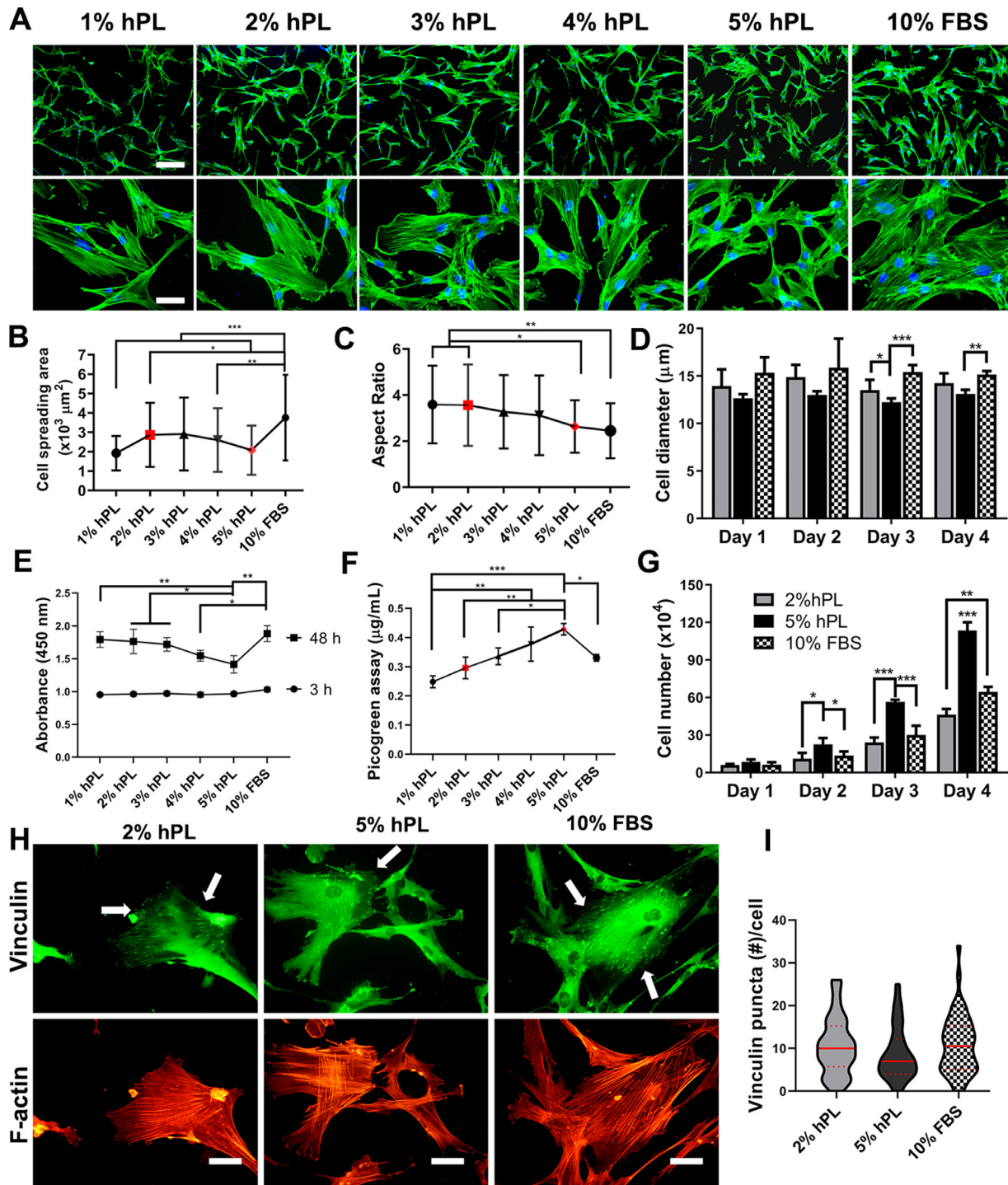


**Fig. 1.** fBMSCs adhesion, proliferation, and morphology in hPL. (A) F-actin (green) staining images of fBMSCs. Scale bars are 200 (top) and 50  $\mu\text{m}$  (bottom), respectively. Quantitative comparison of fBMSCs morphology in different media by spreading area (B), aspect ratio (C), as well as cell diameter in suspension (D). Cell proliferation assay by CCK-8 assay (E), DNA quantification (F), and cell number counting (G) at indicated time points. (H) Vinculin (green) and F-actin (red) staining images of fBMSCs in different media at 48 h. Scale bar is 50  $\mu\text{m}$ . (I) Semi-quantitative comparison of vinculin puncta per cell based on the images in H. Statistical significances were expressed as \* ( $p < 0.05$ ), \*\* ( $p < 0.01$ ), or \*\*\* ( $p < 0.001$ ), respectively.

### 3.5. hPL induced a widespread transcriptome change

After a 7-day culture, fBMSCs in 5% hPL and 10% FBS exhibited significantly different transcriptome expression profiles, as demonstrated by the two-dimensional principal component analysis (PCA) (Fig. S2). A total of 1843 different transcripts were discovered between 5% hPL (hPL-7d) and 10% FBS -cultured fBMSCs (FBS-7d), with 773 up-regulated and 1070 down-regulated (Fig. 5A). The top

20 enriched KEGG pathways include metabolic, PI3K-Akt signaling pathway, focal adhesion, TGF-beta signaling pathway, ECM-receptor interaction and et al. (Fig. 5B).

The transcriptional expression of makers associated with mesenchymal phenotype (e.g. MCAM, VEGFA, FGF2, and LIF) were all downregulated in hPL-fBMSCs (Fig. 5C). On the contrary, the chondrogenic markers such as COMP, ACAN, and COL11A1 were downregulated for 5.33-, 369.8-, and 7.62-folds, whereas the adipogenic

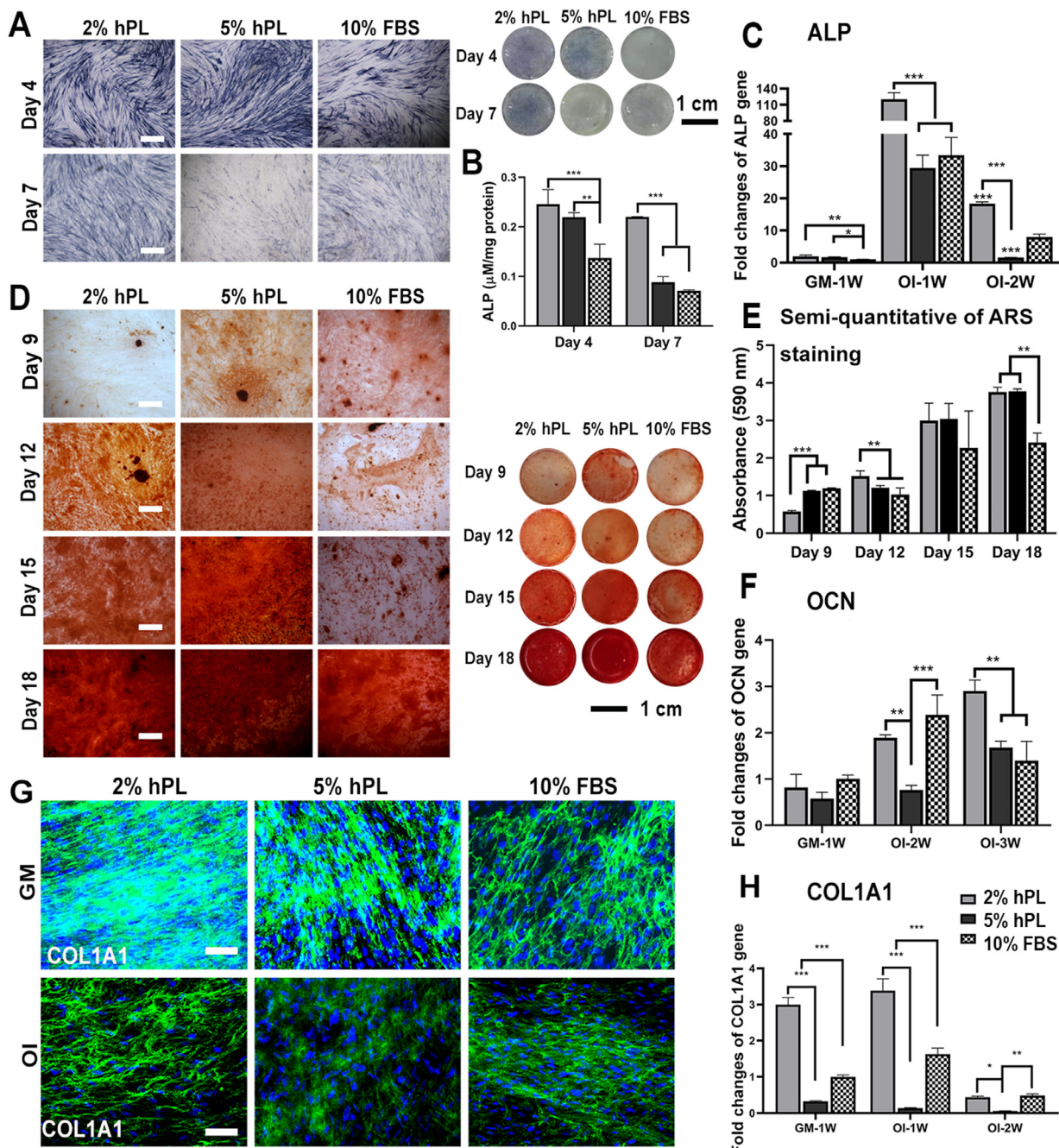


**Fig. 2.** Osteogenic differentiation of fBMSCs in hPL. Staining (A) and quantitative examination (B) of ALP activity in fBMSCs after OI for 4- and 7-days, respectively. Photographs (D) and semi-quantitative analysis (E) of ARS staining of fBMSCs after OI for different periods. Transcriptional level examination of ALP (C), OCN (F), and COL1A1 (H) expressions. (G) COL1A1 staining (green) of fBMSCs in GM and OI media for 7-, and 14-days, respectively, and cell nuclei were stained with DAPI (blue). GM is growth media, and OI is osteogenic induction. Scale bars in A, D, and G are 500  $\mu$ m, 1 cm, and 100  $\mu$ m, respectively. Statistical significances among different test groups were expressed as \* ( $p<0.05$ ), \*\* ( $p<0.01$ ), or \*\*\* ( $p<0.001$ ), respectively.

markers such as PPARG, MMP1, and SFRP1 were up-regulated for 3.58-, 32.50-, and 2.11-folds in 5% hPL-MSCs compared with cells in 10% FBS, respectively. Furthermore, the osteogenic-commitment markers, such as BMP4 and ALPL were upregulated for 3.89-folds, 1.53-folds in 5% hPL-fBMSCs, respectively (Fig. 5D).

### 3.6. hPL altered the PI3K-Akt/HIF-1 pathway and mitochondrial features

According to KEGG enrichment analyses, 56 and 116 out of 1843 DEGs (differently expressed genes) were identified in PI3K-Akt and metabolic pathways, respectively, and both pathways ranked in the

top three by p-value and the count number of DEGs (Fig. 5B). Thus, we speculated that the bioactive factors and nutrients in hPL altered the nutrient-sensing PI3K-Akt/HIF-1 signaling pathway in fBMSCs (Fig. 6A and Fig. S3). To test this hypothesis, we investigated the expression level of HIF1A, the PI3K-Akt downstream transcription factor. It was found that the gene and protein expression of HIF1A in 5% hPL-fBMSCs was down-regulated for about 2- and 2.6-folds (Fig. 6B and 6C) compared with those in 10% FBS-fBMSCs at day 7, respectively.

We next examined the influence of different media supplements on mitochondrial morphology by mitotracker staining. 5%

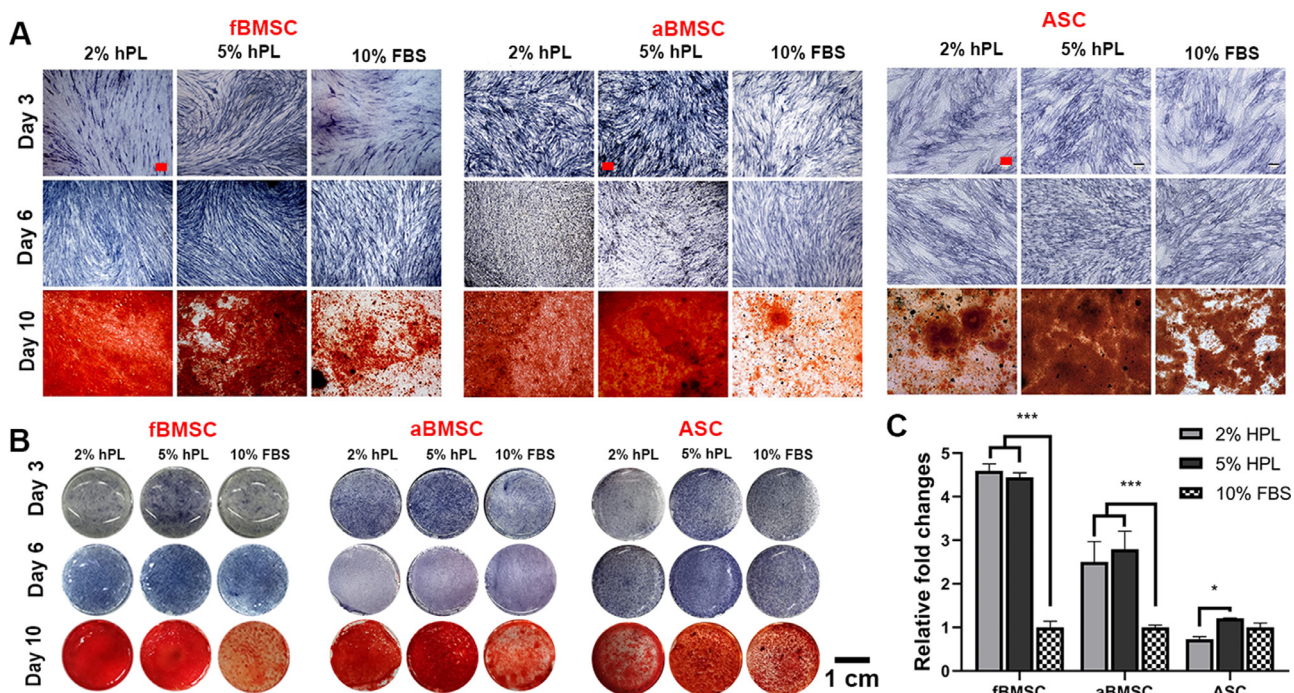


**Fig. 3.** Osteogenic effect of hPL on MSCs from different origins. Photographs (A) and gross images (B) of ALP and ARS staining of MSCs after osteogenic induction for 3, 6, and 10 days, respectively. Scale bars in A and B are 500  $\mu$ m and 1 cm, respectively. (C) Semi-quantitative analysis of ARS staining ( $n$  is 3). Statistical significances were expressed as \* ( $p < 0.05$ ) or \*\*\* ( $p < 0.001$ ), respectively.

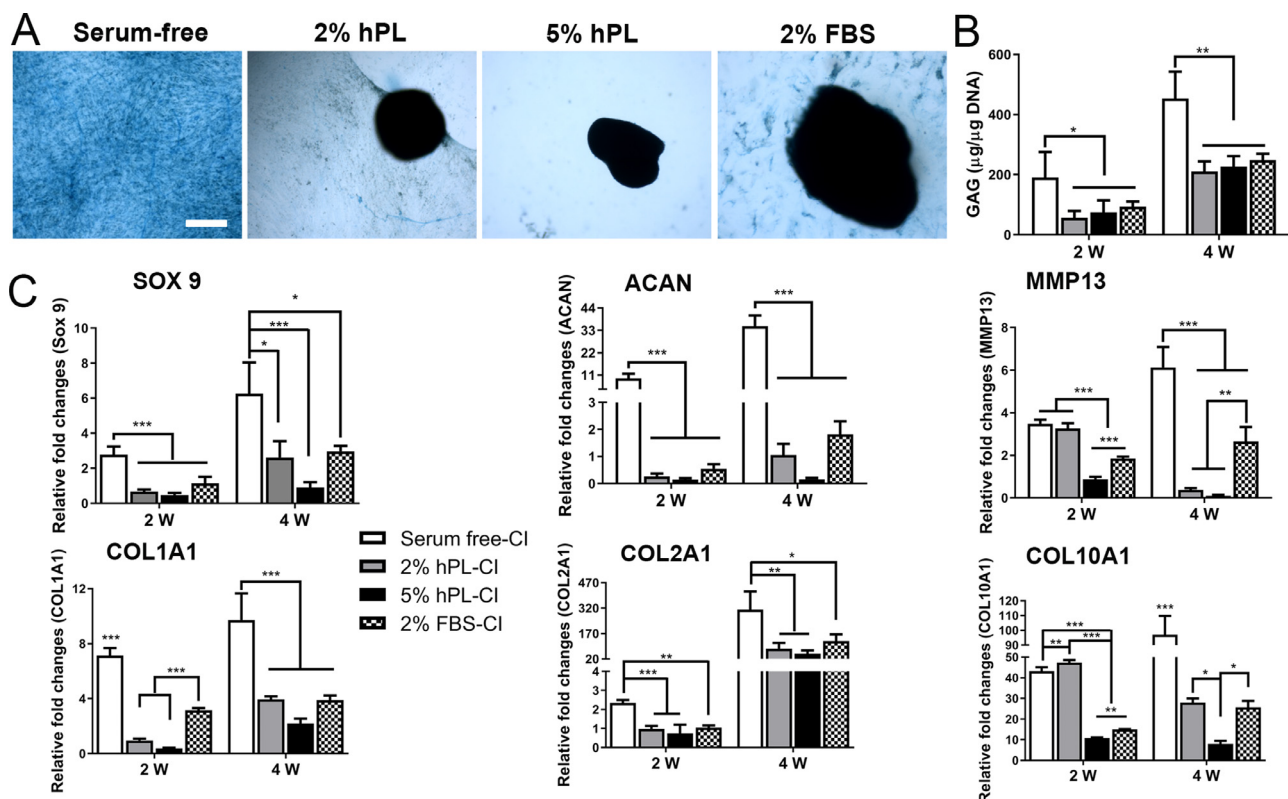


**Fig. 4.** Chondrogenic differentiation of fBMSCs in hPL. (A) Alcian blue staining of fBMSCs after chondrogenic induction (CI) for 4 weeks. Scale bar is 500  $\mu$ m. (B) GAG assay ( $\mu$ g/ $\mu$ g DNA) showed the highest GAG secretion of fBMSCs in serum-free condition. (C) Transcriptional level examination of SOX9, ACAN, MMP13, COL1A1, COL2A1, and COL10A1 after CI for 2- and 4- weeks, respectively.  $n$  is 3 for all experiments. Statistical significances were expressed as \* ( $p < 0.05$ ), \*\* ( $p < 0.01$ ), or \*\*\* ( $p < 0.001$ ), respectively.

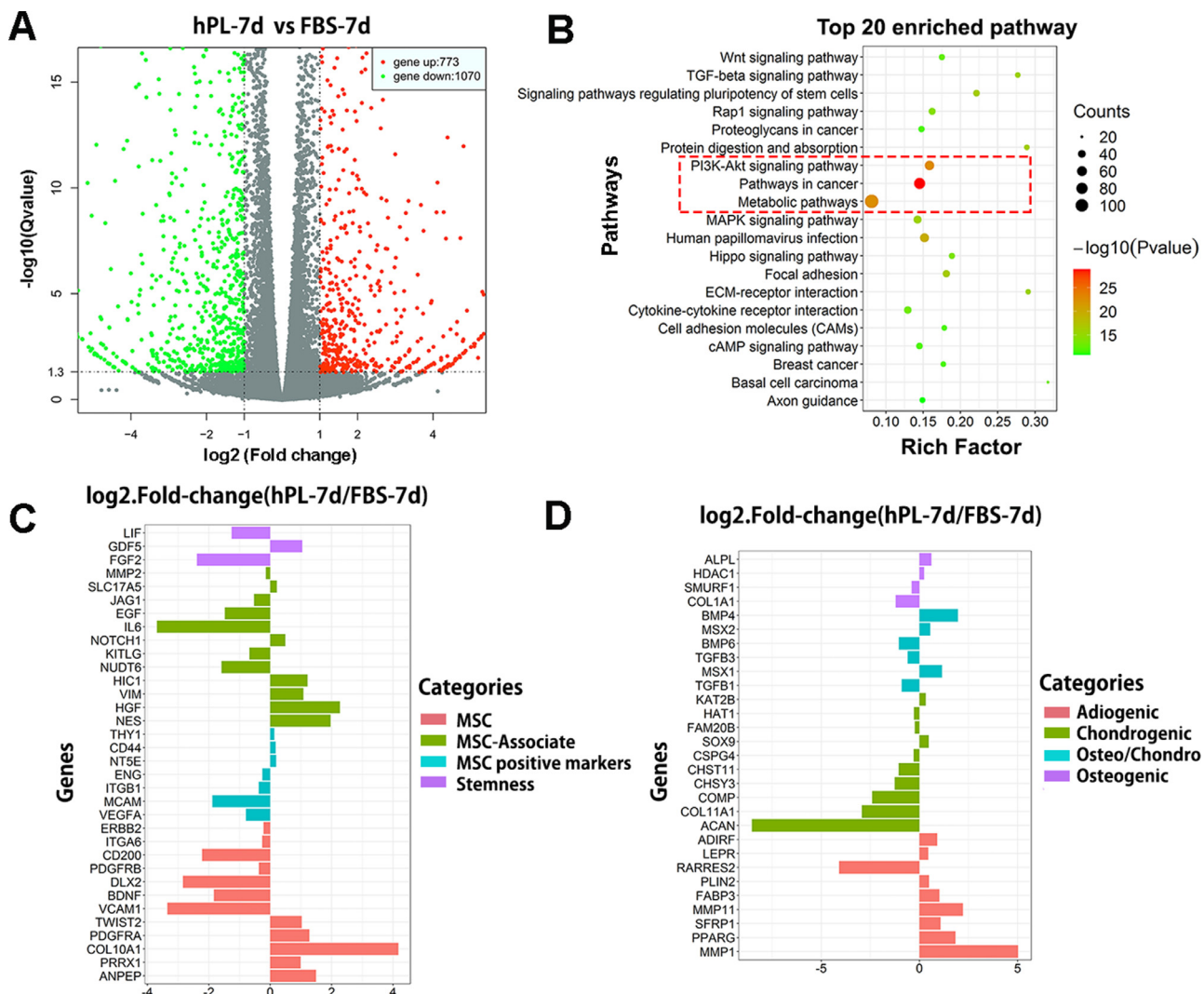


**Fig. 5.** Transcriptome comparison of 5% hPL- and 10% FBS- fBMSCs after they cultured in growth media (GM) for 7 days ( $n = 3$ ), respectively. (A) Volcano plots the total number of genes identified by RNA sequencing. DEGs were defined as  $|log_2(fold\ change)| > 1$ , and  $q\ value < 0.05$  (the up- and down-regulated genes were indicated using red and green dots, respectively). (B) The top 20 enriched KEGG pathways. hPL significantly altered the transcriptional expression of the MSC property- (C) and lineage specification-associated markers (D).

hPL-treated MSCs (fBMSCs and ASCs) exhibited elongated and interconnected mitochondrial networks, which were significantly different from the sparse and fragmented mitochondria in 10% FBS-MSCs (Fig. 6D). Finally, the images and flow cytometry assay of JC-1 staining both demonstrated a reduced mitochondrial membrane potential in 5% hPL-cultured cells (Fig. 6E and 6F).

### 3.7. hPL impaired the immunomodulatory and angiogenic property

For paracrine function evaluation of fBMSCs, the DEGs that enriched into the GO terms of cytokine, growth factor, and chemokine activities were selected and compared, which demonstrated that most of these genes were down-regulated in the 5% hPL-fBMSCs. Specifically, the gene expressions of angiogenic factors (EGF, PDGFA, FGF2, FGF11, and FGF14) and immunomodulatory factors (IL6, IL11, CXCL2, and TNFSF15) were all downregulated in 5% hPL-fBMSCs (Fig. 7A).

At last, a functional activity test of the conditioned media (CM) obtained from hPL- and FBS-fBMSCs was carried out. The results showed that with the treatment of CM for 24 h, M0 macrophage exhibited an obvious morphological change in FBS-CM compared with the cells treated by hPL-CM (Fig. 7B). The secretary-protein

levels of TNF- $\alpha$  and IL-10 of the M0 treated by hPL-CM were relatively lower than cells treated by FBS-CM. In addition, with the treatment of different CM, M1 macrophage did not show any significant changes with cell morphology and IL-10 secretion; however, the TNF- $\alpha$  secretary levels of M1 macrophage were reduced with the treatment by FBS-CM (Fig. 7C and 7D).

Photographs of HUVECs morphology on Matrigel®-coated substrates in different media demonstrated that FBS-CM had a better effect on HUVECs tube formation (Fig. 7E). Quantitative analysis of the total segment lengths further confirmed the better angiogenic effect of FBS-CM than hPL-CM (Fig. 7F). The CCK-8 assay of HUVECs cultured in different CM further validated the advanced promotion effect of FBS-CM on HUVECs proliferation over hPL-CM (Fig. 7G).

## 4. Discussion

This work demonstrated that hPL had a promotive effect on osteogenic differentiation, whilst had an inhibitory effect on chondrogenic differentiation of MSCs. We also comprehensively explored the modulating effect of hPL on MSCs behaviors such as adhesion, morphology, proliferation, immunophenotypes (Fig. S4), cell size, ECM secretion, immunomodulatory, and angiogenic func-

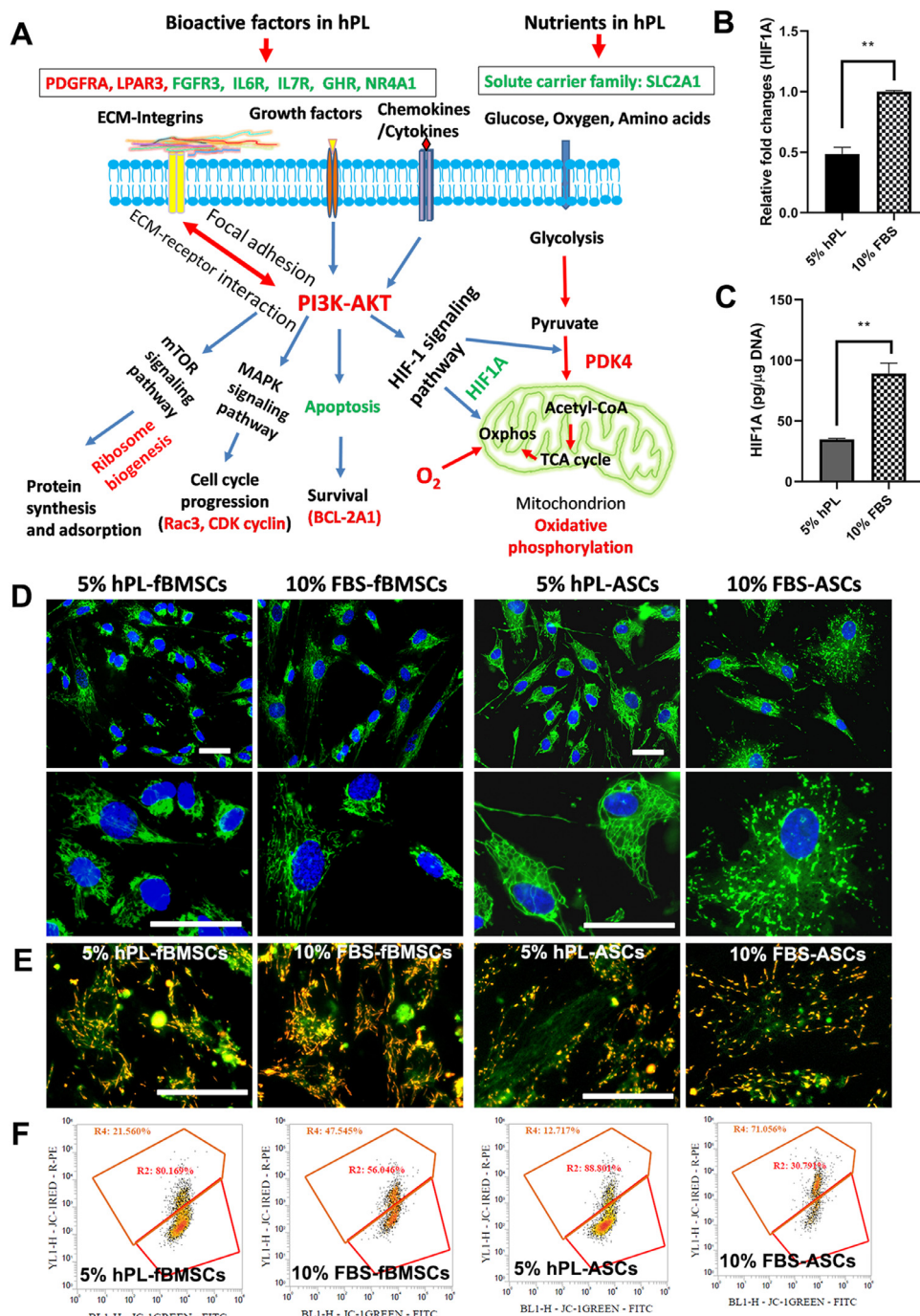


**Fig. 6.** hPL altered the PI3K-Akt/HIF-1 pathway and the mitochondrial features. (A) The bioactive factors and nutrients in hPL altered fBMSCs behaviors via the PI3K-Akt/HIF-1 signaling pathway and the downstream energy metabolism. Transcriptional (B) and protein (C) level expressions of HIF1A in 5% hPL- and 10% FBS-fBMSCs after 7-day culture in GM. (D) Mitochondrial morphology observation by mitotracker staining. Mitochondrial membrane potential was evaluated by JC-1 staining images (E) and flow cytometry assay (F). Scale bars in D and E are 500  $\mu$ m.

tions. Most importantly, we discovered many interesting information regarding the critical signaling pathways of hPL in regulating cellular responses of fBMSCs.

First of all, we found a promotive effect of hPL on fBMSC proliferation in a dose-dependent manner. This effect on various MSCs has been reported previously [24–27]. However, the cell activity measured by CCK-8 assay was inversely correlated with cell number determined by DNA quantification and cell counting, which indicates that the cell activity per cell in hPL is lower than that in FBS (Fig. 1). This result also indicates a possible metabolic change

of fBMSC in hPL, as CCK-8 assay reflects the combinational effect of cell number, medium glucose supply, and cellular glucose metabolic activity. It was reported that the inhibition of glucose transport, metabolic enzyme, and EGFR-PI3K-Akt pathway all suppress WST-8 reduction [28]. The high enrichment of DEGs in the PI3K-Akt and metabolic pathways further implied the metabolic change of hPL-fBMSCs (Fig. 5B). It has been known that the cellular behaviors of MSCs, including proliferation, metabolism, differentiation, and cytokine production, were all modulated by the PI3K-Akt signaling pathway [29]. It is then reasonable to hypothesized that

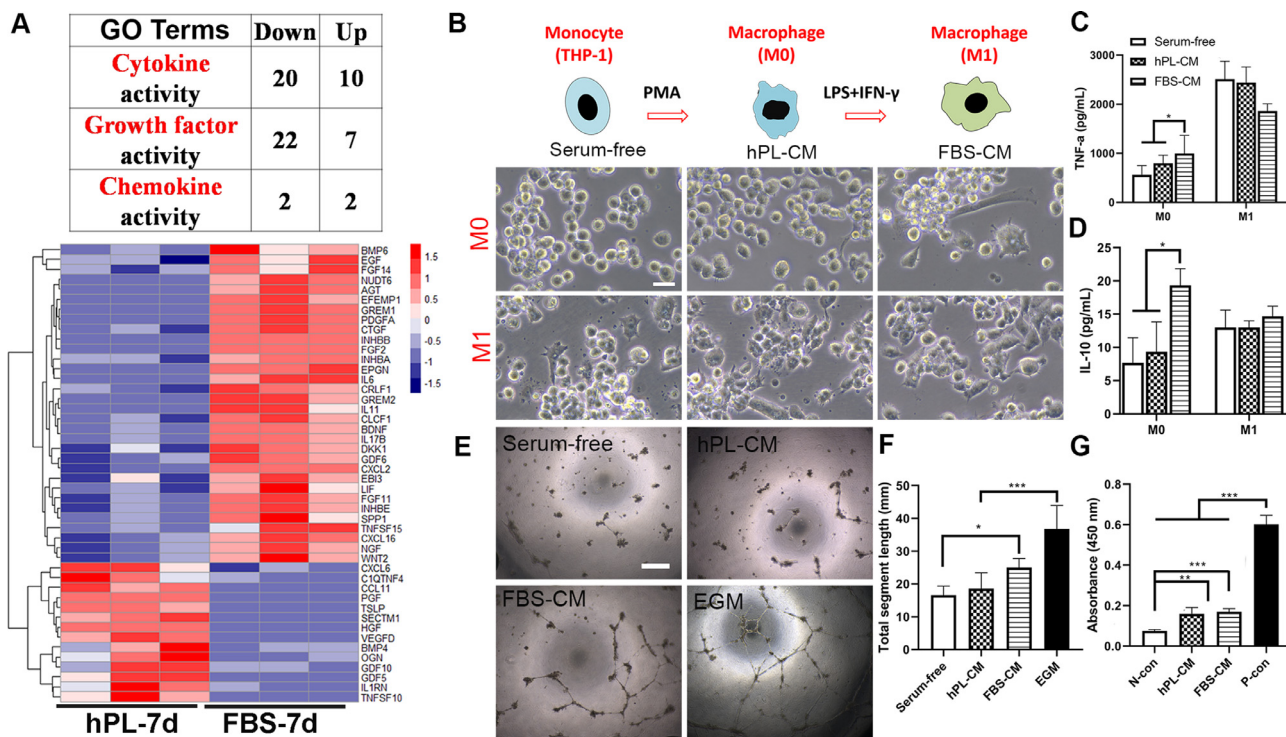


**Fig. 7.** Immunomodulatory and angiogenic properties of fBMSCs in hPL. (A) Heatmap image compared the relative expression of paracrine factors in 5% hPL- and 10% FBS-fBMSCs. (B) Cell morphology of the resting macrophage (M0) and stimulated macrophage (M1) after the treatment with serum-free media, hPL-CM, and FBS-CM, respectively. Secretory-level of TNF- $\alpha$  (C) and IL-10 (D) by M0 and M1 macrophage determined by ELISA after the treatment for 24 h, respectively. (E) HUVECs morphology on Matrigel-coated substrates in different media at 16 h. Quantitative comparison of total segment length (F), and CCK-8 assay (G) of HUVECs after a 24 h-culture in different media. Scale bars in B and E are 50 and 500  $\mu$ m, respectively. Statistical significances were expressed as \* ( $p < 0.05$ ), \*\* ( $p < 0.01$ ), or \*\*\* ( $p < 0.001$ ), respectively.

the abundant growth factors and cytokines in hPL [30] have influenced the PI3K-Akt signaling pathway. For these reasons, we investigated the expression of HIF1A, the PI3K-Akt downstream transcription factor, which is critical in regulating the metabolic fate and multipotency of MSCs [31]. The downregulation of HIF1A in gene and protein levels (Fig. 6B and 6C) indicated the suppression of glycolysis while upregulation of OxPhos in hPL-fBMSCs [32]. Furthermore, RNA sequencing also revealed that genes regulating glycolysis (HIF1A, PGK1, ENO2, and ALDOC) were all down-regulated, while genes regulating mitochondrial OxPhos (NADH dehydrogenases) were all up-regulated in 5% hPL-fBMSCs (Fig. S5).

Given the central importance of mitochondrial metabolism on stem cell function and differentiation [33], we then compared the ultrastructure and membrane potential of mitochondria of MSCs (fBMSCs and ASCs) cultured in different media. The elongated and interconnected mitochondrial networks in hPL-MSCs (Fig. 6D, 6E and 6F) indicated an energy metabolism switch from glycolysis towards mitochondrial OxPhos [34]. The enhanced OxPhos further increased the production of reactive oxygen species (ROS), which probably induced the destabilization of the mitochondrial membrane potential [35] (Fig. 6E and 6F). In addition, the perinuclear distribution of mitochondrial networks (Fig. 6D) may correlate with the reduced cytoskeleton networks in hPL-MSCs (Fig. 1A and Fig. S6), as a previous report showed that the mitochondrial structure was regulated by actin cytoskeletal arrangement [36].

The finding about the metabolic change of MSCs in hPL is critical as recent studies found that the metabolic features play a critical role in directing MSCs self-renewal, multilineage differentiation [37, 38], and immunomodulatory functions [39]. It was reported that bone marrow-MSCs resided in hypoxic niches [40], and these stem cells maintained a high glycolytic metabolism, where differentiating cells undergo a metabolic switch to enhanced OxPhos to drive ATP production [41]. Accordingly, we claimed that the decreased expression of MSC phenotype associated genes and the

increased expression of lineage specification genes of hPL-fBMSCs (Fig. 5C and 5D) were probably induced by the enhanced OxPhos [42, 43]. On the other hand, the inhibitory effect of hPL on fBMSCs chondrogenic differentiation is probably attributed to its suppression on glycolysis, as previous studies reported that the hypoxic environment was more supportive for chondrogenic differentiation [44–46] (Fig. 8).

The finding that fBMSCs in hPL had a more elongated cell morphology and less spreading area than cells in FBS control (Fig. 1B and 1C) is consistent with previous work [47]. Our study for the first time showed that the cell diameter of suspended fBMSCs was significantly reduced in hPL compared with those in the FBS (~13.5%, Fig. 1E). This is significant as it is a substantial decrease in cell volume (~35%). Previous study demonstrated that cell size is vital for cellular function; however, the questions of how cell size is determined and regulated were yet poorly understood [48]. Nevertheless, it is generally accepted that cell size is controlled by both growth rate and cell cycle duration, which is ultimately modulated by the mitochondrial metabolism [49].

RNA sequencing revealed a substantially decreased number of paracrine function-related genes in hPL-fBMSCs, and the functional activity test of CM further corroborated the compromised immunomodulatory and angiogenic effect of hPL-fBMSCs (Fig. 7). The paracrine function of MSCs can be regulated by different molecular mechanisms. It was documented that the telomerase associated protein, Rap1, can significantly affect the paracrine profile of MSCs via NF- $\kappa$ B signaling [50]. However, according to RNA sequencing analysis, there were no significant changes with telomerase-related transcripts in hPL-MSCs compared with FBS-MSCs. HIF-1 signaling pathway is another pivotal intracellular signaling mechanism that regulates important biological events [51]. The significantly downregulated HIF-1 signaling pathway (Fig. S7) explained the decreased pleiotropic paracrine and immunomodulatory functions of hPL-MSCs.

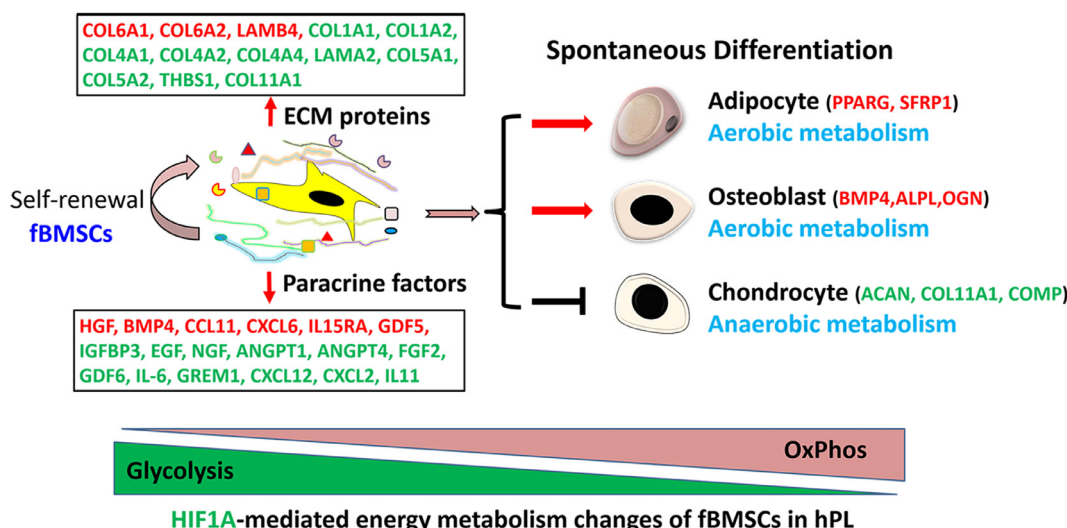


**Fig. 8.** The lineage specification of fBMSCs in 5% hPL is determined by the energy metabolic state. The enhanced OxPhos of fBMSCs in 5% hPL committed them towards the aerobic metabolism-demanded cells (e.g. adipocytes and osteocytes) rather than the anaerobic metabolism-demanded cells (e.g. chondrocytes). In the meantime, the paracrine factor- and ECM component-related genes of fBMSCs were mostly downregulated with 5% hPL treatment.

To investigate whether the osteogenic promotion effect of hPL was caused by the nutrients deficiency or not, we then investigated the osteogenic effect of 0% hPL (i.e. serum-free MEM alpha media). Results showed that 0% hPL failed to support cell propagation or matrix mineralization (Fig. S8), while hPL with a low concentration of 2% was sufficient to induce a significant increase in cell number and matrix mineralization on fBMSC (Fig. 2). All these results suggested that the abundant bioactive components in hPL altered the nutrient-sensing PI3K-Akt signaling pathway that sequentially influenced cellular differentiation and functions (Fig. 6A). However, the downregulation of PI3K-Akt/HIF1A activity in hPL-fBMSCs is against a previous study that PDGF, rich in hPL, is an important factor to activate PI3K-Akt pathway via PDGFR binding [52]. We have tried to examine the protein expression levels of PI3K, and our preliminary results showed that the expression of PI3K is dynamic in hPL-fBMSCs. Further studies are needed to investigate the time-dependent expression of critical proteins involved in the PI3K-Akt/HIF-1 signaling pathway.

Finally, although we have identified some interesting changes of MSCs with the hPL treatment, there are some other limitations with our current work. First, the switched metabolic state of MSCs should be further measured by Agilent Seahorse XF Cell Mito Stress Test Kit [53], and further investigations are needed to understand the molecular mechanisms of hPL on mitochondrial function in MSCs. Second, we could not find the exact different secretion components in the conditioned media of hPL- and FBS-MSCs, a detailed characterization of the secreted components such as protein and extracellular vesicles of MSCs with or without hPL treatment would give more valuable instructions for their therapeutic application [54]. At last, to avoid the batch-to-batch variations in MSCs quality, the pluripotent stem cell-derived MSCs are preferred for future investigations [55].

## Conclusion

This study elucidates the effect of hPL, an ideal xeno-free alternative in the production of clinical-grade cells, on MSCs. In hPL, MSCs are smaller, grow faster, and have a higher osteogenic differentiation efficiency. The downregulated HIF1A in 5% hPL-MSCs inhibited glycolysis but enhanced OxPhos in mitochondria, leading to a preferred lineage commitment towards aerobic metabolism-demanded osteocytes and adipocytes. This finding implied the

great potential of hPL-MSC for bone and fat tissue engineering. On the other hand, the impaired MSC properties in hPL, such as immunomodulatory and angiogenic functions, suggested that hPL-MSCs might not be suitable for treating inflammatory- and ischemic-diseases. This study gives important information on the modulating mechanisms of hPL on MSCs behavior and paracrine function that could give instructions for future application of hPL-MSCs in tissue engineering and regenerative medicine.

## Declaration of Competing Interest

The authors declare that they have no known competing financial interests or personal relationships that could have appeared to influence the work reported in this paper.

## Data availability

The data supporting the findings of this study are available within the paper and its Supplementary Information file. All the RNAseq raw data has been deposited at NCBI Sequence Read Archive (SRA) with the BioProject code PRJNA771770.

## Acknowledgments

Authors thank the funding supports from the Ministry of Science and Technology of China (2019YFE0113000); the National Natural and Science Foundation of China (31900958, 31870988, and 81703090); the Department of Science and Technology of Guangdong Province (2021A0505030055); the Science, Technology, and Innovation Commission of Shenzhen (JCYJ20180302150015952, 20180928115804736 and ZDSYS20190902093409851).

## References

- [1] M.F. Pittenger, A.M. Mackay, S.C. Beck, R.K. Jaiswal, R. Douglas, J.D. Mosca, et al., Multilineage potential of adult human mesenchymal stem cells, *Science* 284 (1999) 143–147.
- [2] M. Abbasi-Kangvari, S.H. Ghamari, F. Safaeinejad, S. Bahrami, H. Niknejad, Potential Therapeutic Features of Human Amniotic Mesenchymal Stem Cells in Multiple Sclerosis: Immunomodulation, Inflammation Suppression, Angiogenesis Promotion, Oxidative Stress Inhibition, Neurogenesis Induction, MMPs Regulation, and Remyelination Stimulation, *Front. Immunol.* 10 (2019) 238.
- [3] K. Drela, L. Stanaszek, A. Nowakowski, Z. Kuczynska, B. Lukomska, Experimental Strategies of Mesenchymal Stem Cell Propagation: Adverse Events and Potential Risk of Functional Changes, *Stem Cells Int.* 2019 (2019) 7012692.

- [4] D.T. Shih, T. Burnouf, Preparation, quality criteria, and properties of human blood platelet lysate supplements for ex vivo stem cell expansion, *New Biotechnol.* 32 (2015) 199–211.
- [5] M. Cimino, R.M. Goncalves, C.C. Barrias, M.C.L. Martins, Xeno-Free Strategies for Safe Human Mesenchymal Stem/Stromal Cell Expansion: Supplements and Coatings, *Stem Cells Int.* 2017 (2017) 6597815.
- [6] A. Oikonomopoulos, W.K. van Deen, A.R. Manansala, P.N. Lacey, T.A. Tomakili, A. Ziman, et al., Optimization of human mesenchymal stem cell manufacturing: the effects of animal/xeno-free media, *Sci. Rep.* 5 (2015) 16570.
- [7] T. Burnouf, D. Strunk, M.B.C. Koh, K. Schallmoser, Human platelet lysate: Replacing fetal bovine serum as a gold standard for human cell propagation? *Biomaterials* 76 (2016) 371–387.
- [8] C. Doucet, I. Ernou, Y. Zhang, J.R. Llense, L. Begot, X. Holy, et al., Platelet lysates promote mesenchymal stem cell expansion: a safety substitute for animal serum in cell-based therapy applications, *J. Cell. Physiol.* 205 (2005) 228–236.
- [9] I. Muller, S. Kordowich, C. Holzwarth, C. Spano, G. Isensee, A. Staiber, et al., Animal serum-free culture conditions for isolation and expansion of multipotent mesenchymal stromal cells from human BM, *Cytotherapy* 8 (2006) 437–444.
- [10] M.A. Avanzini, M.E. Bernardo, A.M. Cometa, C. Perotti, N. Zaffaroni, F. Novara, et al., Generation of mesenchymal stromal cells in the presence of platelet lysate: a phenotypic and functional comparison of umbilical cord blood- and bone marrow-derived progenitors, *Haematol.-Hematol.* J. 94 (2009) 1649–1660.
- [11] B.A. Naaijens, H.W.M. Niessen, H.J. Prins, P.A.J. Krijnen, T.J.A. Kokhuis, N. de Jong, et al., Human platelet lysate as a fetal bovine serum substitute improves human adipose-derived stromal cell culture for future cardiac repair applications, *Cell Tissue Res.* 348 (2012) 119–130.
- [12] E. Fernandez-Rebollo, B. Mentrup, R. Ebert, J. Franzen, G. Abagnale, T. Sieben, et al., Human Platelet Lysate versus Fetal Calf Serum: These Supplements Do Not Select for Different Mesenchymal Stromal Cells, *Sci. Rep.* 7 (2017).
- [13] N. Chevallier, F. Anagnostou, S. Zilber, G. Bodivit, S. Maurin, A. Barrault, et al., Osteoblastic differentiation of human mesenchymal stem cells with platelet lysate, *Biomaterials* 31 (2010) 270–278.
- [14] M. Reis, D. McDonald, L. Nicholson, K. Godthardt, S. Knobel, A.M. Dickinson, et al., Global phenotypic characterisation of human platelet lysate expanded MSCs by high-throughput flow cytometry, *Sci. Rep.* 8 (2018) 3907.
- [15] V. Becherucci, L. Piccini, S. Casamassima, S. Bisin, V. Gori, F. Gentile, et al., Human platelet lysate in mesenchymal stromal cell expansion according to a GMP grade protocol: a cell factory experience, *Stem Cell Res. Ther.* 9 (2018) 124.
- [16] J. van den Dolder, R. Mooren, A.P. Vloon, P.J. Stoepling, J.A. Jansen, Platelet-rich plasma: quantification of growth factor levels and the effect on growth and differentiation of rat bone marrow cells, *Tissue Eng.* 12 (2006) 3067–3073.
- [17] O. Kilian, I. Flesch, S. Wenisch, B. Taborski, A. Jork, R. Schnettler, et al., Effects of platelet growth factors on human mesenchymal stem cells and human endothelial cells in vitro, *Eur. J. Med. Res.* 9 (2004) 337–344.
- [18] G. Astori, E. Amati, F. Bambi, M. Bernardi, K. Chieregato, R. Schafer, et al., Platelet lysate as a substitute for animal serum for the ex-vivo expansion of mesenchymal stem/stromal cells: present and future, *Stem Cell Res. Ther.* 7 (2016).
- [19] H. Abdelrazik, G.M. Spaggiari, L. Chiossone, L. Moretta, Mesenchymal stem cells expanded in human platelet lysate display a decreased inhibitory capacity on T- and NK-cell proliferation and function, *Eur. J. Immunol.* 41 (2011) 3281–3290.
- [20] M.E. Bernardo, M.A. Avanzini, C. Perotti, A.M. Cometa, A. Moretta, E. Lenta, et al., Optimization of in vitro expansion of human multipotent mesenchymal stromal cells for cell-therapy approaches: further insights in the search for a fetal calf serum substitute, *J. Cell. Physiol.* 211 (2007) 121–130.
- [21] I.B. Copland, M.A. Garcia, E.K. Waller, J.D. Roback, J. Galipeau, The effect of platelet lysate fibrinogen on the functionality of MSCs in immunotherapy, *Bio-materials* 34 (2013) 7840–7850.
- [22] R. Costa-Almeida, A.R. Franco, T. Pesqueira, M.B. Oliveira, P.S. Babo, I.B. Leonor, et al., The effects of platelet lysate patches on the activity of tendon-derived cells, *Acta Biomater.* 68 (2018) 29–40.
- [23] M. Kirsch, L. Birnstein, I. Pepelenova, W. Handke, J. Rach, A. Seltsam, et al., Gelatin-Methacryloyl (GelMA) Formulated with Human Platelet Lysate Supports Mesenchymal Stem Cell Proliferation and Differentiation and Enhances the Hydrogel's Mechanical Properties, *Bioengineering* 6 (2019).
- [24] E. Fernandez-Rebollo, B. Mentrup, R. Ebert, J. Franzen, G. Abagnale, T. Sieben, et al., Human Platelet Lysate versus Fetal Calf Serum: These Supplements Do Not Select for Different Mesenchymal Stromal Cells, *Sci. Rep.* 7 (2017) 5132.
- [25] H. Hemeda, B. Giebel, W.V. Wagner, Evaluation of human platelet lysate versus fetal bovine serum for culture of mesenchymal stromal cells, *Cytotherapy* 16 (2014) 170–180.
- [26] S.F. Trojahn Kolle, R.S. Oliveri, P.V. Glovinski, M. Kirchhoff, A.B. Mathiasen, J.J. Elberg, et al., Pooled human platelet lysate versus fetal bovine serum-investigating the proliferation rate, chromosome stability and angiogenic potential of human adipose tissue-derived stem cells intended for clinical use, *Cytotherapy* 15 (2013) 1086–1097.
- [27] D. Cholewa, T. Stiehl, A. Schellenberg, G. Bokermann, S. Joussen, C. Koch, et al., Expansion of Adipose Mesenchymal Stromal Cells Is Affected by Human Platelet Lysate and Plating Density, *Cell Transplant.* 20 (2011) 1409–1422.
- [28] L. Xie, Z. Dai, C. Pang, D. Lin, M. Zheng, Cellular glucose metabolism is essential for the reduction of cell-impermeable water-soluble tetrazolium (WST) dyes, *Int. J. Biol. Sci.* 14 (2018) 1535–1544.
- [29] J. Chen, R. Crawford, C. Chen, Y. Xiao, The key regulatory roles of the PI3K/Akt signaling pathway in the functionalities of mesenchymal stem cells and applications in tissue regeneration, *Tissue Eng. Part B Rev.* 19 (2013) 516–528.
- [30] M. Gnechi, Z. Zhang, A. Ni, V.J. Dzau, Paracrine mechanisms in adult stem cell signaling and therapy, *Circ. Res.* 103 (2008) 1204–1219.
- [31] E. Duval, C. Bauge, R. Andriamananjaoana, H. Benateau, S. Leclercq, S. Dutout, et al., Molecular mechanism of hypoxia-induced chondrogenesis and its application in in vivo cartilage tissue engineering, *Biomaterials* 33 (2012) 6042–6051.
- [32] L.B. Buravkova, E.R. Andreeva, V. Gogvadze, B. Zhivotovsky, Mesenchymal stem cells and hypoxia: where are we? *Mitochondrion* 19 (Pt A) (2014) 105–112.
- [33] M. Khacho, R.S. Slack, Mitochondrial activity in the regulation of stem cell self-renewal and differentiation, *Curr. Opin. Cell Biol.* 49 (2017) 1–8.
- [34] H.C. Chen, D.C. Chan, Mitochondrial Dynamics in Regulating the Unique Phenotypes of Cancer and Stem Cells, *Cell Metab.* 26 (2017) 39–48.
- [35] Q.Q. Li, Z.W. Gao, Y. Chen, M.X. Guan, The role of mitochondria in osteogenic, adipogenic and chondrogenic differentiation of mesenchymal stem cells, *Protein & Cell* 8 (2017) 439–445.
- [36] J.Y. Ye, E.Y. Liang, Y.S. Cheng, G.C.F. Chan, Y. Ding, F.Y. Meng, et al., Serotonin Enhances Megakaryopoiesis and Proplatelet Formation via p-Erk1/2 and F-Actin Reorganization, *Stem Cells* 32 (2014) 2973–2982.
- [37] Y. Liu, T. Ma, Metabolic regulation of mesenchymal stem cell in expansion and therapeutic application, *Biotechnol. Prog.* 31 (2015) 468–481.
- [38] A. Wanet, T. Arnould, M. Najimi, P. Renard, Connecting Mitochondria, Metabolism, and Stem Cell Fate, *Stem Cells Dev.* 24 (2015) 1957–1971.
- [39] R. Contreras-Lopez, R. Elizondo-Vega, M.J. Paredes, N. Luque-Campos, M.J. Torres, G. Tejedor, et al., HIF1 alpha-dependent metabolic reprogramming governs mesenchymal stem/stromal cell immunoregulatory functions, *Faseb J* 34 (2020) 8250–8264.
- [40] S. Palomaki, M. Pietila, S. Laitinen, J. Pesala, R. Sormunen, P. Lehenkari, et al., HIF-1alpha is upregulated in human mesenchymal stem cells, *Stem Cells* 31 (2013) 1902–1909.
- [41] M. Khacho, R.S. Slack, Mitochondrial activity in the regulation of stem cell self-renewal and differentiation, *Curr. Opin. Cell Biol.* 49 (2017) 1–8.
- [42] C.T. Chen, Y.R. Shih, T.K. Kuo, O.K. Lee, Y.H. Wei, Coordinated changes of mitochondrial biogenesis and antioxidant enzymes during osteogenic differentiation of human mesenchymal stem cells, *Stem Cells* 26 (2008) 960–968.
- [43] Y. Zhang, G. Marsboom, P.T. Toth, J. Rehman, Mitochondrial respiration regulates adipogenic differentiation of human mesenchymal stem cells, *PLoS One* 8 (2013) e77077.
- [44] V. Zubillaga, A. Alonso-Varona, S.C.M. Fernandes, A.M. Salaberria, T. Palomares, Adipose-Derived Mesenchymal Stem Cell Chondrospheroids Cultured in Hypoxia and a 3D Porous Chitosan/Chitin Nanocrystal Scaffold as a Platform for Cartilage Tissue Engineering, *Int. J. Mol. Sci.* 21 (2020).
- [45] C. Galeano-Garces, E.T. Camilleri, S.M. Riester, A. Dudakovic, D.R. Larson, W.C. Qu, et al., Molecular Validation of Chondrogenic Differentiation and Hypoxia Responsiveness of Platelet-Lysate Expanded Adipose Tissue-Derived Human Mesenchymal Stromal Cells, *Cartilage* 8 (2017) 283–299.
- [46] Y. Yao, J. Shang, W. Song, Q. Deng, H. Liu, Y. Zhou, Global profiling of the gene expression and alternative splicing events during hypoxia-regulated chondrogenic differentiation in human cartilage endplate-derived stem cells, *Genomics* 107 (2016) 170–177.
- [47] K. Schallmoser, C. Bartmann, E. Rohde, A. Reinisch, K. Kashofer, E. Stadelmeyer, et al., Human platelet lysate can replace fetal bovine serum for clinical-scale expansion of functional mesenchymal stromal cells, *Transfusion* 47 (2007) 1436–1446.
- [48] M. Bjorklund, Cell size homeostasis: Metabolic control of growth and cell division, *Biochimica et biophysica acta Mol. Cell Res.* 1866 (2019) 409–417.
- [49] T.P. Miettinen, M. Bjorklund, Mitochondrial Function and Cell Size: An Allometric Relationship, *Trends Cell Biol.* 27 (2017) 393–402.
- [50] Y. Zhang, S. Chiu, X. Liang, F. Gao, Z. Zhang, S. Liao, et al., Rap1-mediated nuclear factor-kappaB (NF-kappaB) activity regulates the paracrine capacity of mesenchymal stem cells in heart repair following infarction, *Cell Death Discovery* 1 (2015) 15007.
- [51] H.S. Shi, S.Y. Yang, S.H. Zeng, X. Liu, J. Zhang, J. Zhang, et al., Enhanced angiogenesis of biodegradable iron-doped octacalcium phosphate/poly(lactic-co-glycolic acid) scaffold for potential cancerous bone regeneration, *Appl. Mater.: Today* 15 (2019) 100–114.
- [52] J.Y. Ye, G.C.F. Chan, L.A. Qiao, Q.Z. Lian, F.Y. Meng, X.Q. Luo, et al., Platelet-derived growth factor enhances platelet recovery in a murine model of radiation-induced thrombocytopenia and reduces apoptosis in megakaryocytes via its receptors and the PI3-k/Akt pathway, *Haematol.-Hematol.* J. 95 (2010) 1745–1753.
- [53] D. Jiang, G. Xiong, H. Feng, Z. Zhang, P. Chen, B. Yan, et al., Donation of mitochondria by iPSC-derived mesenchymal stem cells protects retinal ganglion cells against mitochondrial complex I defect-induced degeneration, *Theranostics* 9 (2019) 2395–2410.
- [54] A. Thakur, X. Ke, Y.W. Chen, P. Motallebnejad, K. Zhang, Q. Lian, et al., The mini player with diverse functions: extracellular vesicles in cell biology, disease, and therapeutics, *Protein & Cell* (2021).
- [55] A.J.C. Bloor, A. Patel, J.E. Griffin, M.H. Gilleece, R. Radia, D.T. Yeung, et al., Production, safety and efficacy of iPSC-derived mesenchymal stromal cells in acute steroid-resistant graft versus host disease: a phase I, multicenter, open-label, dose-escalation study, *Nat. Med.* 26 (2020) 1720–1725.